Journal of Applied Polymer Science

Effects of Rare Earth Samarium Oxide on the Properties of Polypropylene-*Graft*-Cardanol Grafted by Reactive Extrusion

Xinggong Mao,[1] Yi Deng,[1] Jinhuo Lin,[1,2] Qinhui Chen[1,2]
[1]College of Materials Science and Engineering, Fujian Normal University, Fuzhou 350007, China
[2]Fujian Key Laboratory of Polymer Materials, Fuzhou 350007, China
Correspondence to: Q. Chen (E-mail: chenqh@fjnu.edu.cn)

ABSTRACT: Rare earth elements can improve the performance of polymers because of their special 4f orbitals. The nucleation and stabilization of radical groups of rare earth particles can affect the structure of polypropylene (PP) and its properties. In this study, samarium oxide (Sm_2O_3) particles were used as a cocatalyst and nucleating agent in polypropylene-*graft*-cardanol (CAPP) grafted by reactive extrusion. The properties of polypropylene-*graft*-cardanol containing modified Sm_2O_3 with a titanate coupling agent (CAPPMS) were investigated by ultraviolet–visible spectrometry, polarizing microscopy, differential scanning calorimetry, scanning electron microscopy, universal testing, and capillary rheometry with the reference of CAPP containing unmodified Sm_2O_3 particles. The results show that the titanate coupling agent (TCA-401) coated on the surface of the Sm_2O_3 particles improved the dispersion of the Sm_2O_3 particles and the adhesion between the Sm_2O_3 particles and CAPP matrix. The Sm_2O_3 particles promoted more cardanol to graft onto PP. Acting as nucleator for CAPP, the Sm_2O_3 particles increased the crystallization rate, increased the melting temperature, and decreased the spherulite size of CAPP. The modified Sm_2O_3 particles showed a greater effect on the mechanical and rheological properties than the unmodified Sm_2O_3 particles did. The tensile strength, impact strength and flexural strength of CAPPMS increased by 10 MPa, 0.64 kJ/m^2, and 6.5 MPa, respectively, compared to those of CAPP when we used 4.5 mol % modified Sm_2O_3 particles. The viscosity of CAPPMS increased to a certain extent in the presence of the modified Sm_2O_3. © 2014 Wiley Periodicals, Inc. J. Appl. Polym. Sci. **2014**, *131*, 41012.

KEYWORDS: crystallization; extrusion; grafting; polyolefins

Received 24 January 2014; accepted 12 May 2014
DOI: 10.1002/app.41012

INTRODUCTION

Nowadays, to improve the surface energy of polypropylene (PP), scientists have spent a lot of time in modification research.[1–6] In particular, the graft modification of reactive extrusion has shown remarkable results and, thus, has aroused widespread interest[7–11] because of its solvent-free properties, continuity in the production process, and ease of reaction time manipulation. However, reactive extrusion causes the decomposition of PP chains in the presence of radical groups. Our former study on polypropylene-*graft*-cardanol (CAPP) showed that cardanol (CNSL) grafted onto PP improved the surface energy of PP and inhibited its degradation during processing, storage, and application[12] because the natural product of CNSL had the dual effect of electron-donating and electron-withdrawing because of the p–π conjugated system of CNSL (Scheme 1). On the other hand, PP is a kind of crystal polymer. Reactive extrusion will affect the crystal structure of PP. The crystal structure of PP is important to the properties of PP. Many inorganic particles have been added to PP to improve its processability and mechanical properties.[13–16]

However, little attention has been paid to rare earth particles added to PP. The rare earth elements, which include Sc, Y, and the 15 lanthanides (La to Lu) have special properties, such as optical, electrical, magnetic, and chemical catalysis and so on, because of their particular electronic structure.[17–19] Most of the rare earth elements are paramagnetic substances because of the 4f orbitals containing parallel-spin unpaired electrons, which are located in the inner space. The 4f orbitals can quickly capture unstable free radicals generated by an initiator because of their good stability. Therefore, rare earth oxide particles can extend the life of the free radicals. Zhu and coworkers[20,21] studied the effect of rare earth compounds in assisting the melt grafting of maleic anhydride onto isotatic PP by reactive extrusion. They found that a series of rare earth oxides could promote the grafting reaction. Herein, in our experiment, rare earth samarium oxide (Sm_2O_3) particles were used as a cocatalyst and nucleating agent for CAPP during reactive extrusion.

It is well known that the surface of unmodified Sm_2O_3 is hydrophilic, whereas the CAPP matrix is hydrophobic. Therefore, the

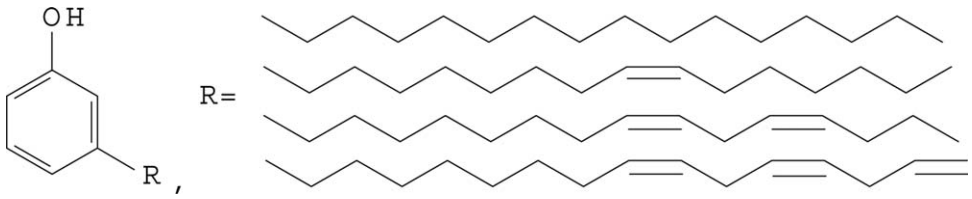

Scheme 1. Molecular structure of CNSL.

surface modification of the Sm_2O_3 particles was necessary to improve the dispersion of the Sm_2O_3 particles in the CAPP matrix and their adhesion.[2,13,22,23] In this study, the properties of polypropylene-*graft*-cardanol containing modified Sm_2O_3 with a titanate coupling agent (CAPPMS) were investigated by ultraviolet–visible (UV–vis) spectrometry, polarizing microscopy (PLM), differential scanning calorimetry (DSC), scanning electron microscopy (SEM), universal testing, and capillary rheometry with a reference of polypropylene-*graft*-cardanol containing unmodified Sm_2O_3 particles (CAPPS).

EXPERIMENTAL

Materials

Isotactic PP (PPH-XD-045, melt flow index = 2.1–6.0 g/10 min) was purchased from Shandong Kairi Chemical Industry, Ltd., Co. (China). The initiator, dicumyl peroxide (DCP), was supplied by Sinopharm Chemical Reagent. The monomer, CNSL, was purchased from a local market without any further purification. Sm_2O_3 particles with diameters of 50–500 nm were purchased from Shandong Zhuoqun Rare Earth, Ltd., Co. (China). A tetraisopropyl di(dioctylphosphate) titanate coupling agent (TCA-401) was supplied by Nanjing Nengde Chemical Industry, Ltd., Co. (China). All other reagents were analytical grade.

Surface Modification of the Sm_2O_3 Particles

An amount of 10 g of predried Sm_2O_3 particles and 0.8 g of TCA-401 dissolved in 60 mL of isopropyl alcohol were put into a three-necked flask. After ultrasonic dispersion, the three-necked flask was moved into a water bath at 80°C with stirring and maintained for 3 h. Finally, the surface-modified Sm_2O_3 particles were gathered by filtering, rinsing with isopropyl alcohol, and drying in a vacuum oven at 70°C for 12 h.

Preparation of CAPPMS and CAPPS

A certain ratio of Sm_2O_3 particles, PP, CNSL, and DCP (Table I) was mixed and extruded by a corotating twin-screw extruder (Haake Polylab Rheomix PTW24/28, Germany) at a temperature of 170–190°C and at a screw rotation speed of 50 rpm. Then, the extrudates were pelletized after water cooling. The pellets were dried in an oven at 50°C for 12 h. The coarse products of CAPPMS by reactive extrusion were obtained. The coarse products were purified by dissolution in refluxing xylene and then precipitation into acetone under constant stirring to remove the unreacted CNSL. The precipitate was filtered and rinsed with acetone and dried in a vacuum oven at 50°C overnight. The samples used in the mechanical property measurements were prepared by an injection-molding machine (JN55E, China) with temperatures of 185, 190, and 185°C from the feeding zone to the die. The injection was done at a pressure of 30 MPa for 10 s, and the cooling time was 20 s. CAPPS was obtained by the same method and at the same ratios as CAPPMS.

Characterization

Fourier Transform Infrared (FTIR) Measurements. The IR spectra were analyzed by a Nicolet-5700 Fourier transform infrared spectrometer with KBr pellets to determine whether the TCA-401 was grafted onto the surface of the Sm_2O_3 particles.

UV–Vis Spectroscopy Measurement. The concentration of CNSL grafted onto PP was quantified by a UV–vis spectrometer (PerkinElmer, Lambda850). A standard curve was decided by the absorbance unit thickness of a series of PP films containing quantified CNSL at 273 nm. The grafting ratio was decided by the absorbance unit thicknesses of the purified CAPPS and CAPPMS.

Crystallization Behavior. ***PLM measurement.*** The spherulite morphologies of CAPP, CAPPS, and CAPPMS were observed with a Leica DMLP polarizing microscope mounted on a Linkam TM600 hot stage. The purified samples were first heated to 210°C at a rate of 30°C/min and then cooled to 130°C at the same rate. The temperature was kept constant for 10 min. At the same time, the crystallization processes were photographed to judge the difference between the spherulites.

DSC measurement. The crystalline and melting behaviors of CAPP, CAPPS, and CAPPMS were studied by DSC (Mettler TGA/SDTA851). About 4–7 mg of the purified sample was first heated quickly to 220°C and then kept for 5 min to eliminate the thermal history. Later, it was cooled at a rate of 10°C/min. When the temperature reached to 50°C, it was reheated again to 220°C at a heating rate of 10°C/min. The crystalline and melting parameters were recorded from the cooling and heating thermograms.

SEM measurement. The brittle fractured surfaces of CAPP, CAPPS, and CAPPMS were observed by SEM (JSM-7500F,

Table I. Formulation of CAPPMS by Reactive Extrusion

	PP (portion)	CNSL (portion)	DCP (portion)	Sm_2O_3 (mmol)
CA-PPMS$_{1.5}$	100	5	0	1.5
CAPPMS$_0$	100	5	0.2	0.0
CAPPMS$_{1.5}$	100	5	0.2	1.5
CAPPMS$_{3.0}$	100	5	0.2	3.0
CAPPMS$_{4.5}$	100	5	0.2	4.5
CAPPMS$_{6.0}$	100	5	0.2	6.0
CAPPMS$_{7.5}$	100	5	0.2	7.5

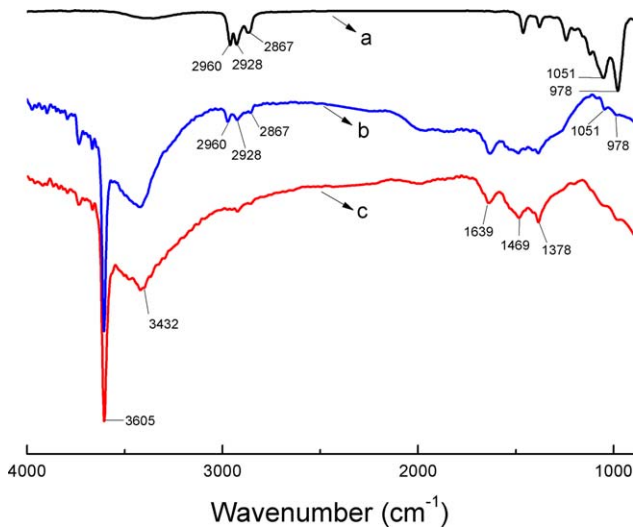

Figure 1. FTIR spectra of (a) TCA-401, (b) modified Sm_2O_3 particles, and (c) unmodified Sm_2O_3 particles. [Color figure can be viewed in the online issue, which is available at wileyonlinelibrary.com.]

Japan) after the scanned surfaces were vacuum-sputtered with platinum.

Capillary Rheological Property Testing. A single-screw extruder (Haake Polylab, Rheomix 252P, Germany) was used to measure the shear viscosity (a pressure sensor and a temperature transducer were installed at the die inlet) at 200°C. The inner diameter of the capillary die was 1.2 mm, and the capillary die had a length/diameter ratio of 40. The rotation speed varied from 2 to 100 rpm in logarithmic form. An automatic data-collection system was used to analyze the test results.

Mechanical Property Measurement. The dumbbell-shaped specimens of CAPP, CAPPS, and CAPPMS were used for the tensile strength and elongation at break testing with a universal testing machine (LLOYD LR 5k, United Kingdom) at a crosshead speed of 20 mm/min. The flexural strength was also obtained by the same machine at a crosshead speed of 20 mm/min and with a span length of 60 mm with the method of three-point bending. The impact strength was measured on an impact testing machine (JJ-20, China) with the method of a simple support beam. Each result was collected as an average value of five samples.

RESULTS AND DISCUSSION

FTIR Spectra

The FTIR spectra of the TCA-401, modified Sm_2O_3 particles, and unmodified Sm_2O_3 particles are shown in Figure 1. There was a broad, strong absorption band at 3432 cm^{-1} related to the stretching vibrations of the —OH group, as shown in Figure 1(c). This indicated the presence of —OH groups on the surface of the unmodified Sm_2O_3 particles. After the Sm_2O_3 particles were modified with TCA-401, significant new bands in the region 3000–2800 cm^{-1}, as shown in Figure 1(b), were associated with the asymmetric and symmetric stretching vibrations of $—CH_3$ and $—CH_2$ groups, which were not observed in Figure 1(c). Moreover, there were two weak characteristic absorptions at 1051 and 978 cm^{-1}, as shown in Figure 1(b), due to the stretching vibrations of the P—O and P═O bonds of TCA-401.

Figure 2. Hydrophobic test of unmodified Sm_2O_3 particles (left) and modified Sm_2O_3 particles (right). [Color figure can be viewed in the online issue, which is available at wileyonlinelibrary.com.]

To discover the effects of the modification of TCA-401 on the Sm_2O_3 particles, a hydrophobic test was carried out by the dispersion of unmodified and modified Sm_2O_3 particles into water. Figure 2 clearly shows that the unmodified Sm_2O_3 particles could disperse in the water, whereas the modified Sm_2O_3 particles could be completely suspended on the surface of the water. The hydrophilic surface of the Sm_2O_3 particles was transformed into a hydrophobic surface after modification. This confirmed the reaction between the TCA-401 and Sm_2O_3 particles, and a possible reaction mechanism[24] is shown in Scheme 2.

Effect of the Sm_2O_3 Concentration on the Grafting Ratio of CAPPS and CAPPMS

The effects of the Sm_2O_3 concentration on the grafting ratio of CAPPS and CAPPMS are illustrated in Figure 3. We found that the grafting ratio increased with the increasing Sm_2O_3 concentration. Under the same experimental conditions, the grafting ratio of a mixture of polypropylene and cardanol in the absence of the dicumyl peroxide initiator (CA-$PPMS_{1.5}$) without DCP initiator was zero; this indicated that only Sm_2O_3 could not induce the grafting reaction. The free radicals decomposed by

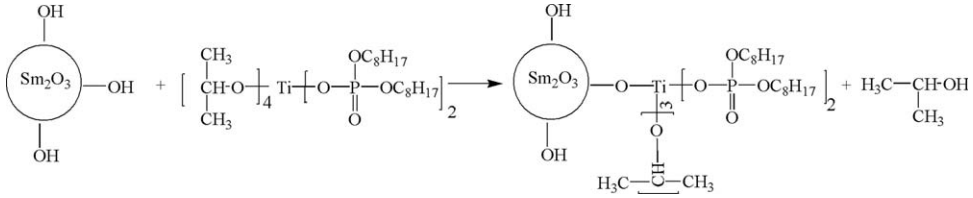

Scheme 2. Possible mechanism of the reaction of Sm_2O_3 particles with TCA-401.

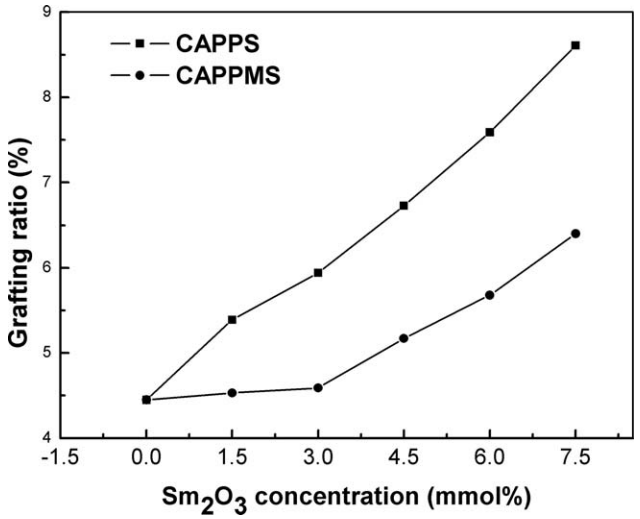

Figure 3. Effect of the Sm_2O_3 concentration on the grafting ratio of CAPPS and CAPPMS.

DCP terminated in various ways because of their unpaired electrons, unless they could quickly initiate the macroradicals of PP and CNSL.[25,26] Sm_2O_3 is a paramagnetic substance because of the 4f orbitals of Sm(III) containing five parallel-spin unpaired electrons. As a result, a certain amount of free radicals were preferentially stabilized by Sm_2O_3; this could be explained by the synergistic effect[20,21] between DCP and Sm_2O_3. A metastable complex[21] composed of Sm_2O_3 and free radicals was formed. However, the bond formation of the metastable complex was too weak to break under heating and shear force conditions during the process of reactive extrusion. Then, free radicals were released anew to abstract hydrogen atoms from the PP and CNSL chains to form the macroradicals. In this way, first, the larger the amount of longeval free radicals in the reactional system was, the higher the concentration of macroradicals formed for the grafting reaction was. In addition, Sm_2O_3 also stabilized macroradicals, which made them more longeval and efficient for the grafting reaction during the process of reactive extrusion. At the same time, the β decomposition of the tertiary macroradicals for PP were also inhibited to some extent, and the degradation of the PP matrix was reduced.[27] Therefore, the grafting ratio of CAPP increased with the increase of Sm_2O_3 concentration.

The TCA-401 coated on the surface of the Sm_2O_3 particles weakened the effect of the 4f orbitals. In addition, the stereohindrance effect of the long alkyl chains of TCA-401 resulted in the fact that the grafting ratio of CAPPMS was lower than that of CAPPS. During reactive extrusion, Sm_2O_3 was equivalent to a cocatalyst in improving the grafting ratio of CAPP.

Crystalline Behavior

Figure 4 clearly shows the crystalline morphologies of CAPP, CAPPS, and CAPPMS. The crystalline structures were spherulitic for all of the samples. The size of the spherulites decreased in the presence of Sm_2O_3. Meanwhile, the boundary of the spherulites became indistinct with increasing Sm_2O_3 concentration. The Sm_2O_3 particles could be used as nucleating agents; this induced the formation of a quantity of spherulites. The spherulitic structure became imperfect because of the quick nucleation and continuous impingement of small spherulites. The Sm_2O_3 particles acted as nucleating agents and promoted the crystalline rate and changed the morphology of the spherulites.

Figure 5(a,b) depicts the respective cooling and melting DSC curves of CAPP, CAPPS, and CAPPMS. The crystallization temperatures of CAPPS were higher than those of CAPP. However, the crystallization temperatures of CAPPMS were similar to

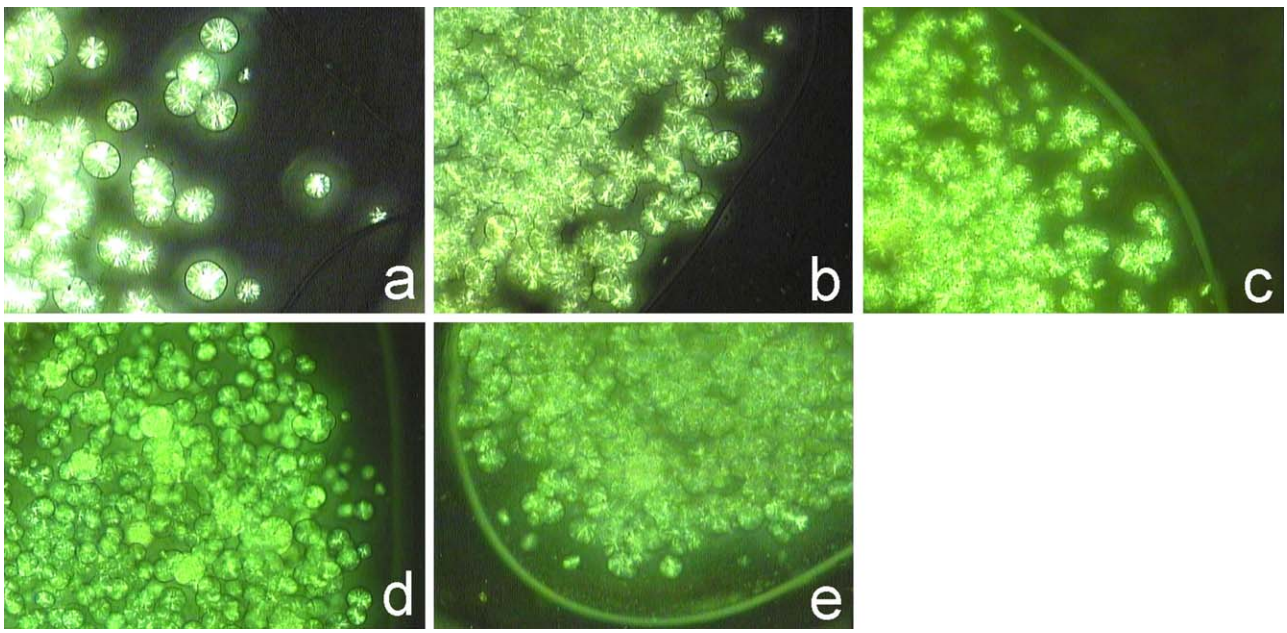

Figure 4. PLM images of (a) CAPP, (b) $CAPPS_{1.5}$, (c) $CAPPS_{7.5}$, (d) $CAPPMS_{1.5}$, and (e) $CAPPMS_{7.5}$ with the same crystalline time of 4 min at 130°C. [Color figure can be viewed in the online issue, which is available at wileyonlinelibrary.com.]

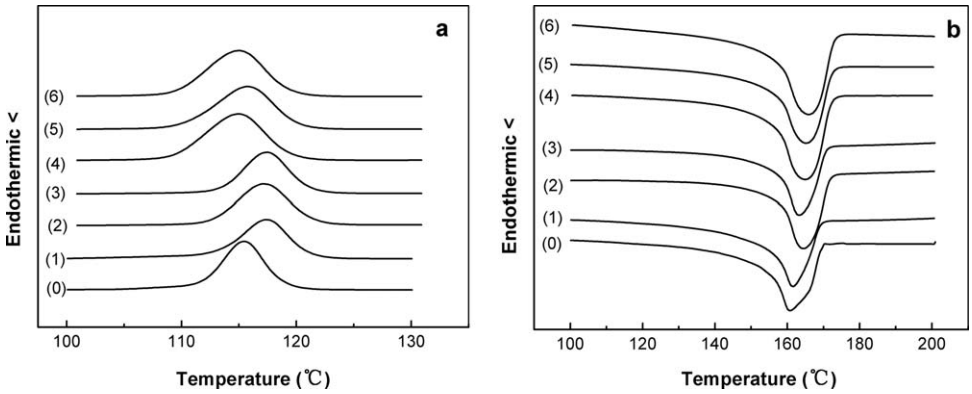

Figure 5. (a) DSC cooling thermograms and (b) melting thermograms of (0) CAPP, (1) $CAPPS_{1.5}$, (2) $CAPPS_{4.5}$, (3) $CAPPS_{7.5}$, (4) $CAPPMS_{1.5}$, (5) $CAPPMS_{4.5}$, and (6) $CAPPMS_{7.5}$.

those of CAPP. This indicated that the unmodified Sm_2O_3 particles possessed better nucleation than the modified Sm_2O_3 particles and could induce CAPP to crystallize at a higher temperature. The melting peak of CAPP could be divided into two endothermic peaks [Figure 5(b)]. The low melting temperature was attributed to the α_1 crystal phase (big spherulites) and the high melting temperature was associated with the α_2 crystal phase[13,28] (small spherulites), respectively. With the addition of the Sm_2O_3 nucleating agent, the ratio of the α_2 crystal phase increased, so the melting peaks of CAPPS transferred to higher temperatures compared to those of CAPP. Because of the overlapping α_1 and α_2 crystal phases, the melting peaks of CAPPMS were broader than those of CAPP.

Morphology of the Brittle Fractured Surfaces

Figure 6 shows the morphologies of the brittle fractured surfaces of CAPP, CAPPS, and CAPPMS. CAPP showed a rough surface morphology with small dimples. White particles were obvious in the brittle fractured surface of CAPPS because of the agglomeration of unmodified Sm_2O_3 particles. However, the modified Sm_2O_3 particles dispersed uniformly in the CAPP matrix. There were more accidented zones and bigger dimples on the CAPPMS surface than on the CAPPS surface. This was attributed to the coupling agent coated on the surface of the Sm_2O_3 particles, which could have lowered the surface energy of the Sm_2O_3 particles and decreased their agglomeration. Moreover, the lipophilic group of TCA-401 enhanced the adhesion between the modified Sm_2O_3 particles and the CAPP matrix to improve the toughness of the material.

Mechanical Properties

The mechanical properties of CAPP, CAPPS, and CAPPMS are shown in Figure 7. In Figure 7(a), the tensile strength of CAPPS was lower by about 2 MPa than that of CAPP. This was due to the poor adhesion between the hydrophilic Sm_2O_3 particles and the CAPP matrix, which produced microcracks because of interface debonding. After the Sm_2O_3 particles were modified with TCA-401, the tensile strength of CAPPMS was much higher than that of CAPP. Moreover, with the increase in the modified Sm_2O_3 concentration, the tensile strength of CAPPMS increased first and reached a maximum value of 10 MPa when the concentration of modified Sm_2O_3 particles was 4.5 mmol %. Then, the tensile strength of CAPPMS dropped gradually when the concentration of modified Sm_2O_3 particles was greater than 6.0 mmol %. The reasons were as follows: (1) more defects existed in the spherulites of CAPP with increasing Sm_2O_3 particle concentration, and (2) the high concentration of fillers increased the distance of the molecular chains, decreased the intermolecular forces, and damaged chain entanglement. The elongation at break of CAPP with Sm_2O_3 particles was worse than that without Sm_2O_3 particles [Figure 7(b)]. This was because the Sm_2O_3 particles restricted the molecular chain movement; this resulted in a drop in the matrix extension. Figure 7(c,d) shows that the improvement of the impact strength and flexural strength were prominent with the addition of modified Sm_2O_3 particles; this was attributed to the good distribution and the similar adhesion between the modified Sm_2O_3 particles and CAPP matrix.

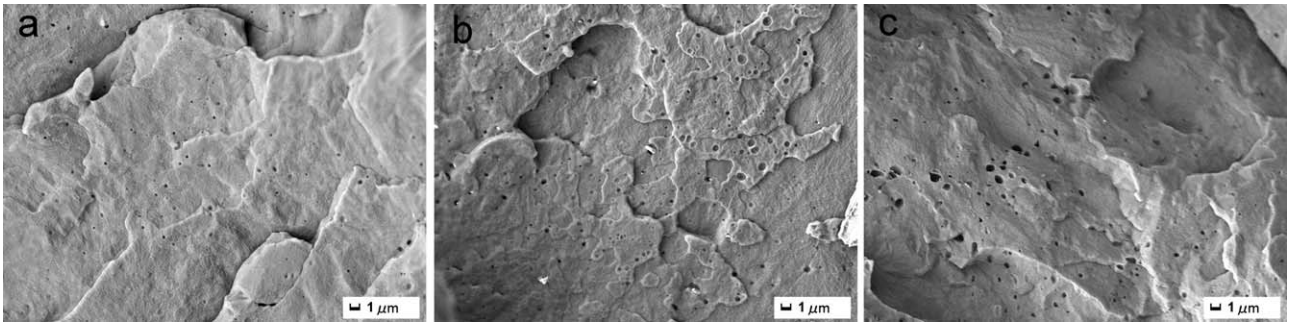

Figure 6. SEM images of (a) CAPP, (b) $CAPPS_{4.5}$, and (c) $CAPPMS_{4.5}$.

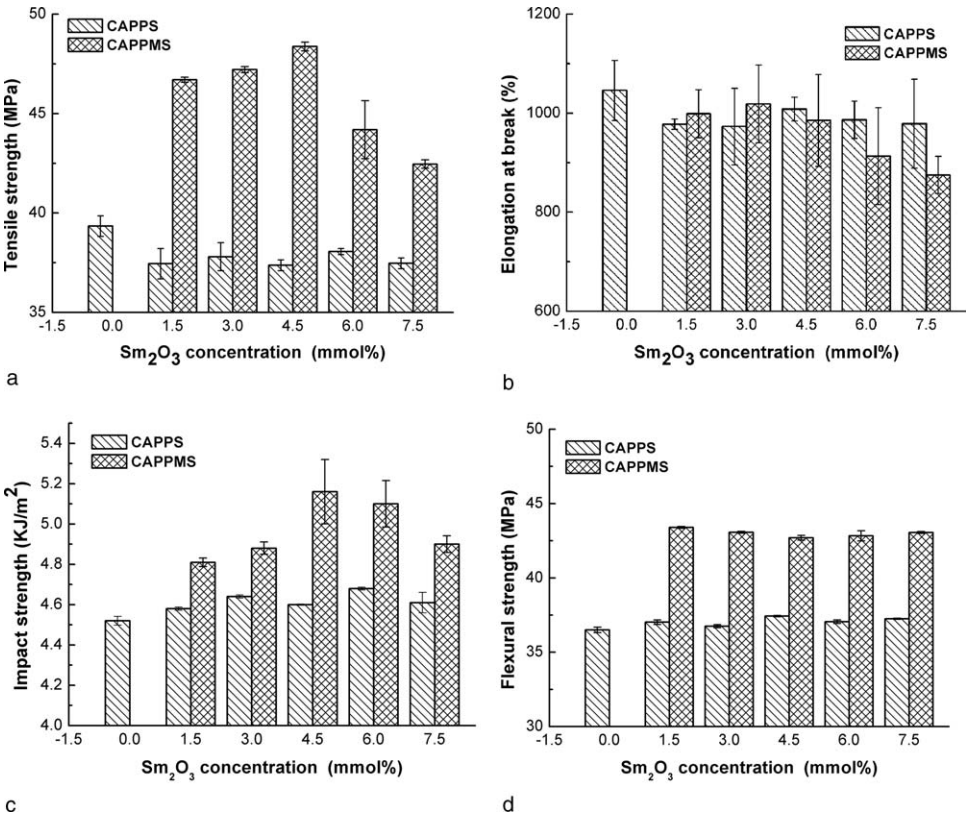

Figure 7. Mechanical properties of CAPP, CAPPS, and CAPPMS.

Capillary Rheological Properties

Capillary rheometry is a useful technique for measuring the shear viscosity for high-viscosity polymers. Generally, the shear rate (γ) and viscosity (η) are correspond to the values in the following equation (1):

$$\eta = K\gamma^{n-1} \quad (1)$$

where K is a parameter related to temperature and n is the non-Newtonian index. When the value of n is low, the non-Newtonian behavior of the material is strong.

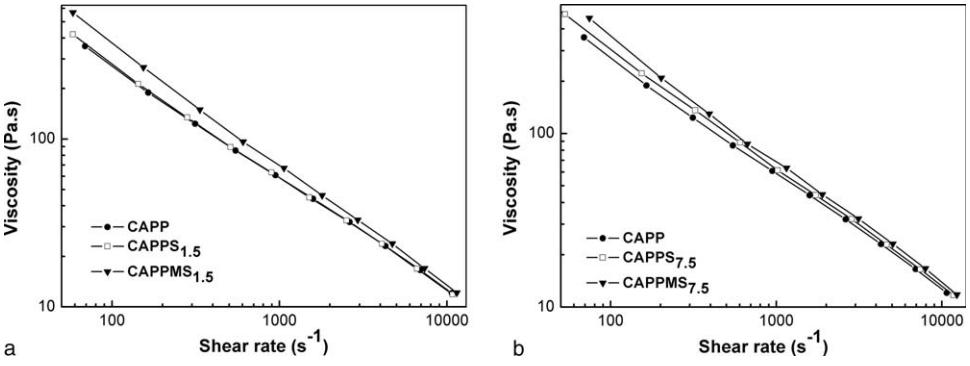

Figure 8. Flow properties of CAPP, CAPPS, and CAPPMS.

Table II. Results for the Capillary Flow Properties

	Unmodified Sm2O3 concentration (mmol %)						Modified Sm2O3 concentration (mmol %)				
	0	1.5	3.0	4.5	6.0	7.5	1.5	3.0	4.5	6.0	7.5
$K \times 10^3$ (Pa s^{-n})	5.60	6.07	6.42	6.87	7.21	7.02	10.00	9.22	9.20	8.92	8.88
n	0.3406	0.3298	0.3233	0.3169	0.3135	0.3192	0.2821	0.2915	0.2917	0.2966	0.2984

Figure 8 shows the capillary flow properties of CAPP, CAPPS, and CAPPMS. CAPPS and CAPPMS are typically pseudoplastic fluids. The viscosity of the fluid decreased with increasing shear rate, which indicated shear-thinning behavior in the polymer. The variation of the viscosity for CAPPS or CAPPMS was more obvious at low shear rate than those at high shear rate.

According to Figure 8(a), the viscosity of $CAPPMS_{1.5}$ (where the subscript indicates the millimolar value of Sm_2O_3 for every 100 g of PP) was much higher than that of CAPP at low shear rate. On the contrary, the viscosity of $CAPPS_{1.5}$ (where the subscript indicates the millimolar value of Sm_2O_3 for every 100 g of PP) was not much different from that of CAPP. This resulted from better adhesion between the modified Sm_2O_3 and CAPP matrix. Just for this reason, the concentration of the modified Sm_2O_3 particles had little influence in the viscosity of CAPPMS. However, with the increase of unmodified Sm_2O_3 particles, the viscosity of CAPPS increased [Figure 8(b)] because of the microphase separation due to the poor interfacial interaction between the unmodified Sm_2O_3 particles and CAPP.

The value of K and n calculated by eq. (1) are illustrated in Table II. We found that the value of K increased but the index of n decreased in the presence of the Sm_2O_3 particles. The K value of CAPPS showed an increasing tendency with an increase in the unmodified Sm_2O_3 particles. On the contrary, the parameter K of CAPPMS decreased with increasing modified Sm_2O_3 particles. At the same Sm_2O_3 particle concentration, the K value of CAPPMS was always higher than that of CAPPS. In addition, the variation in the n value was quite slight at the different Sm_2O_3 concentrations. The index of n of CAPPMS was lower than that of CAPPS.

CONCLUSIONS

CAPP cocatalyzed by Sm_2O_3 particles was prepared by reactive extrusion. TCA-401 coated on the surface of the Sm_2O_3 particles improved the dispersion of the Sm_2O_3 particles and the adhesion between the Sm_2O_3 particles and CAPP matrix. The Sm_2O_3 particles promoted more CNSL to graft onto PP. Acting as nucleators for CAPP, the Sm_2O_3 particles raised the crystallization rate, increased the melting temperature, and decreased the spherulites size of CAPP. The modified Sm_2O_3 particles showed a greater effect on the mechanical and rheological properties than the unmodified Sm_2O_3 particles. The tensile strength, impact strength, and the flexural strength of CAPPMS increased by 10 MPa, 0.64 kJ/m^2, and 6.5 MPa, respectively, compared with those of CAPP when the usage of modified Sm_2O_3 particles was 4.5 mmol %. The viscosity of CAPPMS increased to a certain extent in the presence of modified Sm_2O_3. In conclusion, modified Sm_2O_3 is a promising cocatalyst and nucleating agent, which can be used in PP-*graft*-CNSL during reactive extrusion to enhance the mechanical properties and processability. This opens the way for using various rare earth oxide particles in polymers.

ACKNOWLEDGMENTS

This work was supported by the Natural Science Foundation of China (contract grant number 51103024) and the Fujian Normal University Foundation for Excellent Young Teachers (contract grant number fjsdky2012004).

REFERENCES

1. Varga, J. *Therm. Anal.* **1989**, *35*, 1891.
2. Kazayawoko, M.; Balatinecz, J.; Matuana, L. *J. Mater. Sci.* **1999**, *34*, 6189.
3. Cui, N.-Y.; Brown, N. *Appl. Surf. Sci.* **2002**, *189*, 31.
4. Shim, J. K.; Na, H. S.; Lee, Y. M.; Huh, H.; Nho, Y. C. *J. Membr. Sci.* **2001**, *190*, 215.
5. Shi, D.; Hu, G.-H.; Li, R. *Chem. Eng. Sci.* **2006**, *61*, 3780.
6. Harth, K.; Hibst, H. *Surf. Coat. Technol.* **1993**, *59*, 350.
7. Moad, G. *Prog. Polym. Sci.* **1999**, *24*, 81.
8. Rosales, C.; Perera, R.; Ichazo, M.; Gonzalez, J.; Rojas, H.; Sánchez, A.; Diaz, A. *J. Appl. Polym. Sci.* **1998**, *70*, 161.
9. Bettini, S.; Agnelli, J. *J. Appl. Polym. Sci.* **2002**, *85*, 2706.
10. Lu, H.; Hu, Y.; Li, M.; Chen, Z.; Fan, W. *Compos. Sci. Technol.* **2006**, *66*, 3035.
11. Sun, Y. J.; Hu, G. H.; Lambla, M. *J. Appl. Polym. Sci.* **1995**, *57*, 1043.
12. Chen, Q.; Deng, Y.; Mao, X.; Yin, F.; Lin, J. *J. Appl. Polym. Sci.* **2014**, *131*, DOI: 10.1002/app.39911.
13. Bikiaris, D. N.; Papageorgiou, G. Z.; Pavlidou, E.; Vouroutzis, N.; Palatzoglou, P.; Karayannidis, G. P. *J. Appl. Polym. Sci.* **2006**, *100*, 2684.
14. Wang, S.-W.; Yang, W.; Bao, R.-Y.; Wang, B.; Xie, B.-H.; Yang, M.-B. *Colloid Polym. Sci.* **2010**, *288*, 681.
15. Thwe, M. M.; Liao, K. *Compos. A* **2002**, *33*, 43.
16. Chatterjee, A.; Mishra, S. *Macromol. Res.* **2013**, *21*, 474.
17. Ofelt, G. *J. Chem. Phys.* **1963**, *38*, 2171.
18. Harmon, B. *J. Phys. Colloques* **1979**, *40*, 65.
19. Maestro, P.; Huguenin, D. *J. Alloys Compd.* **1995**, *225*, 520.
20. Zhu, L.; Tang, G.; Shi, Q.; Yin, J. *Chem. J. Chin. Univ.* **2006**, *27*, 970.
21. Zhu, L.; Tang, G.; Shi, Q.; Cai, C.; Yin, J. *J. Polym. Sci. Part B: Polym. Phys.* **2006**, *44*, 134.
22. Sun, S.; Li, C.; Zhang, L.; Du, H.; Burnell-Gray, J. *Eur. Polym. J.* **2006**, *42*, 1643.
23. Fu, S.-Y.; Feng, X.-Q.; Lauke, B.; Mai, Y.-W. *Compos. B* **2008**, *39*, 933.
24. Lin, X.; Zhang, P.; Yin, Z.; Chen, Q. *Chem. World* **2006**, *8*, 454.
25. Chen, Q.; Xue, H.; Lin, J. *J. Appl. Polym. Sci.* **2010**, *115*, 1160.
26. Sun, Y. J.; Hu, G. H.; Lambla, M. *Angew. Makromol. Chem.* **1995**, *229*, 1.
27. Gaylord, N. G.; Mishra, M. K. *J. Polym. Sci: Polym. Lett. Ed.* **1983**, *21*, 23.
28. Boudenne, A.; Ibos, L.; Fois, M.; Gehin, E.; Majeste, J. C. *J. Polym. Sci. Part B: Polym. Phys.* **2004**, *42*, 722.